Remnant of the ancient Farallon Plate breakup: A low-velocity body in the lower oceanic crust off Nicoya Peninsula, Costa Rica - evidence from wide-angle seismics

Christian Walther and Ernst Flueh
GEOMAR Research Center for Marine Geosciences, Kiel, Germany

Received 1 March 2002; revised 3 June 2002; accepted 10 June 2002; published 15 October 2002.

[1] A seismic wide-angle section offshore Costa Rica is presented across the boundary between oceanic crust generated at the East Pacific rise (EPR) and at the Galápagos spreading center (GSC) as indicated by magnetic anomalies. This suture, where the Farallon plate broke up ~23 Ma ago, is marked by pronounced velocity variations throughout the crust including a low-velocity body in the lower crust. This body is well constrained by refracted waves above the inversion zone and by strong P_mP reflections from its lower boundary. The distinctness of this body and the local gravity field point to an igneous intrusion rather than serpentinized rock. Typical oceanic crust is found adjacent to the suture zone. *INDEX TERMS:* 3025 Marine Geology and Geophysics: Marine seismics (0935); 3040 Marine Geology and Geophysics: Plate tectonics (8150, 8155, 8157, 8158); 0930 Exploration Geophysics: Oceanic structures; 9355 Information Related to Geographic Region: Pacific Ocean. **Citation:** Walther, C., and E. Flueh, Remnant of the ancient Farallon Plate breakup: A low-velocity body in the lower oceanic crust off Nicoya Peninsula, Costa Rica - evidence from wide-angle seismics, *Geophys. Res. Lett.*, *29*(19), 1939, doi:10.1029/2002GL015026, 2002.

1. Introduction

[2] The plate tectonic setting in the eastern Pacific off Central America and northern South America is determined by the Cocos and Nazca plates (Figure 1). Both plates are formed at two almost perpendicular spreading centers, the EPR to the west and the GSC between them. The boundary which separates the two different surface expressions of these crustal provinces, smooth EPR and mostly rough GSC crust, can be followed across each plate. This feature was first noted by *Fisher* [1961] and is referred to as the rough-smooth boundary (RSB). The current plate tectonic situation established ~23 Ma ago [*Barckhausen et al.*, 2001], when the former Farallon plate rifted into the Cocos and Nazca plates along a pre-existing zone of weakness, the ancient Grijalva fracture zone (GFZ) [*Hey*, 1977; *Lonsdale and Klitgord*, 1978]. *Hey* [1977] and *Lonsdale and Klitgord* [1978] interpreted the Grijalva scarp off Peru at 3° to 6° S as the southern remnant of this fracture zone, but the location of the northern counterpart long remained unclear. The RSB off Costa Rica, which points towards the southernmost tip of the Nicoya peninsula of Costa Rica was long regarded as a possible location [*von Huene et al.*, 1995]. New magnetic, bathymetric and reflection seismic data off Costa Rica recently led to a revised interpretation of the northeastern counterpart of the GSC-EPR interaction zone [*Barckhausen et al.*, 2001]. The identified magnetic anomalies indicate this boundary as a line, where two magnetic patterns with perpendicular orientations meet. It is located off the center of the Nicoya peninsula and referred as ''fracture zone surface trace'' (FZST) hereafter (Figure 1). NW-SE orientated magnetic anomalies 6B and 6C are found, on EPR crust and border a NE-SW trending anomaly 6B on GSC crust. About 80 km of the FZST are still preserved on the oceanic crust of the Cocos plate, seaward of the Middle America trench (MAT). It coincides with a scarp up to 200 m high, identified in high resolution bathymetry [*von Huene et al.*, 2000] which linked to a volcanic structure on top of the basement (Figure 5).

[3] The above mentioned observations are all constrained by upper crustal features and may be affected through extensive lateral lava flows, such as the sill drilled in this area during ODP leg 170 [*Kimura et al.*, 1997]. To investigate the transition from EPR to GSC domain throughout the whole crust and the upper mantle, a wide-angle seismic section was collected during the PAGANINI cruise of RV SONNE in 1999. We here present the results of this investigation.

2. Wide-Angle Experiment

[4] The 112 km long wide-angle section is located about 40 km seaward of and parallel to the MAT and runs almost perpendicular to the orientation of the FZST (Figure 1). It is coincident with the multi-channel seismic (MCS) line BGR 99-45 [*Barckhausen et al.*, 2001]. According to the interpretation of magnetic data the NW part of the section is situated on ancient Farallon crust formed at the EPR which was about 0.5 to 1 Ma old when the breakup along the GFZ occurred. The SE section runs on crust formed by the GSC. Shots were recorded by 12 ocean-bottom hydrophones (OBH) deployed in about 3300 m waterdepth and at 6 km average spacing. Two 32-litre airguns were used as seismic source; the average shot spacing was 120 m. Data processing included time and offset dependent frequency filtering and deconvolution. All record sections are presented in the PAGANINI cruise report [*Bialas et al.*, 1999].

[5] Data quality varies but is generally good with clear P-wave arrivals up to 70 km offset. The record sections also show PSP-converted phases travelling as P-waves in water and sediment and as S-waves in the basement. The main frequency of the signal lies between 6 and 7 Hz. Despite deconvolution, the signal is characterized by 500 to 800 ms long reverberations. Two representative record sections are displayed in Figures 2a and 2c and show OBH 151 on EPR-derived crust and OBH 159 with its NW section on EPR and its SE section on GSC crust. The identified seismic

0094-8276/02/2002GL015026

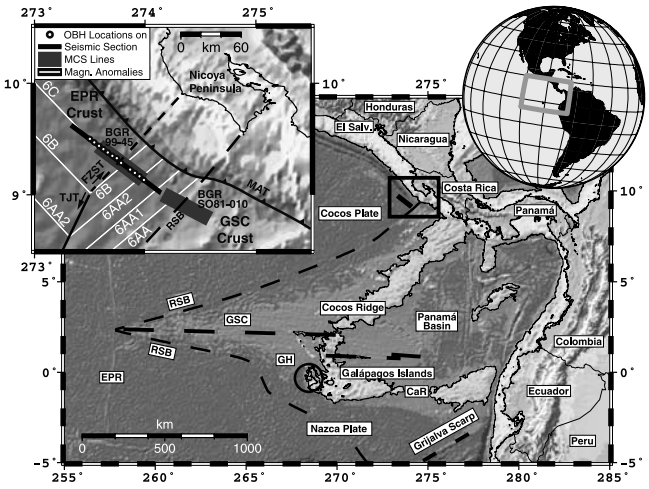

Figure 1. Bathymetric map of the Panamá basin and surrounding area based on satellite altimetry [*Smith and Sandwell*, 1997]. The inset is a close up of the investigated area with the presented PAGANINI seismic wide-angle section. CaR: Carnegie Ridge, EPR: East Pacific Rise, GSC: Galápagos Spreading Center, GH: Galápagos Hotspot, RSB: Rough-Smooth Boundary, FZST: Fracture Zone Surface Trace, TJT: Triple Junction Trace, magnetic anomalies after *Barckhausen et al.* [2001]: 6AA, 6AA1, 6AA2, 6B, 6C.

phases are annotated in Figures 2b and 2d. Sediment thickness and velocity are too low to produce a significant first arrival. The crustal phase can be divided into three individual branches $\mathbf{P_1}$, $\mathbf{P_2}$ and $\mathbf{P_3}$. $\mathbf{P_1}$ and $\mathbf{P_2}$ are refraction, in the upper oceanic crust. $\mathbf{P_3}$ travels through the lower crust and shows a pronounced amplitude decay for branches towards the FZST location at section km 62. The Moho reflection $\mathbf{P_mP}$ is weak in the EPR domain. From OBH 154 on to the SE the energy of the $\mathbf{P_mP}$ increases, indicating a highly reflective crust-mantle boundary SE of the FZST. Simultaneously the critical $\mathbf{P_mP}$ distance reduces to shorter offsets and the phase becomes clearly separated from $\mathbf{P_3}$ (Figure 2c). The phase $\mathbf{P_n}$ from the uppermost mantle is weak but visible on all sections to the NW to the SE $\mathbf{P_n}$ is only observed on OBH 150 to 155.

3. Wide-Angle Model and Discussion

[6] The model is developed for P-waves, basically with the interactive 2-D raytracing program by trial and error. A layer-stripping strategy is applied modeling from top to bottom. A traveltime inversion program is used for fine-tuning the model and assesses the quality of the model providing rms-errors between observed and computed traveltimes for each branch. Reflectivity synthetic modeling is used to test and verify specific model features.

[7] The crustal model is presented in Figure 3 together with the ship gravity and magnetic data collected on cruise BGR 99 (U. Barckhausen, per. com.). The model is based on the inversion of almost 5000 traveltime picks. The achieved traveltime fit is given in Table 1 for all identified branches. Figures 2b and 2d show calculated traveltime branches overlain on record sections OBH 151 and OBH 159. An concrete example for the two-point ray coverage is given in Figure 4 for the most interesting model part. In Figure 5 the coincident MCS line BGR 99-45 is presented [*Barckhausen et al.*, 2001] with the layer interfaces of the wide-angle model superimposed. In the following, the crustal model is described from top to bottom:

[8] A rather uniform sedimentary layer of 400 to 450 m is modeled with velocities between 1.7 and 1.8 km/s. Local basement rises cause thinning of this layer.

[9] The upper crust is modeled with two layers corresponding to the observed phases P_1 and P_2. Velocities in the uppermost basement layer range from 3.3 to 4.2 km/s at the top and 4.8 to 5.6 km/s at the base. Average thickness is 1 km in most parts of the section, but an increase to 2 km depth occurs from 50 km on up to 75 km. The velocity gradient ranges between 0.6 s^{-1} and 1.2 s^{-1}. The lower layer of the upper crust is about 1.3 km thick and average velocities range from 5.8 km/s for the top to 6.4 km/s for the base, with an average gradient of 0.4 s^{-1}.

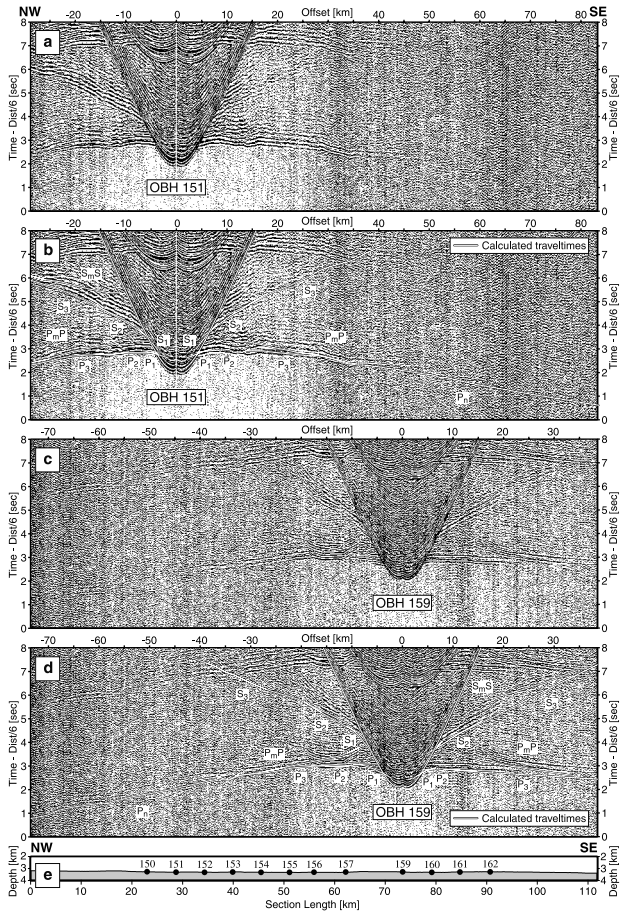

Figure 2. (a) Record section of OBH 151 located in the EPR crustal domain. Time axis is reduced by 6 km/s. (b) Record section with superimposed traveltimes calculated through geometrical raytracing. The nomenclature is as follows: P_1 = refraction in the uppermost crust, P_2 = refraction in the lower part of the upper crust, P_3 = refraction in the lower crust, P_mP = reflection from the crust-mantle boundary, P_n = mantle refraction travelling in the uppermost mantle, the waterwave has no label. S_1, S_2, S_3, S_mS are the corresponding S-wave phases. (c) Record section of OBH 159 located in the transition from the EPR to the GSC crustal domain and (d) with superimposed traveltimes. (e) Sea floor topography and OBH locations along the section.

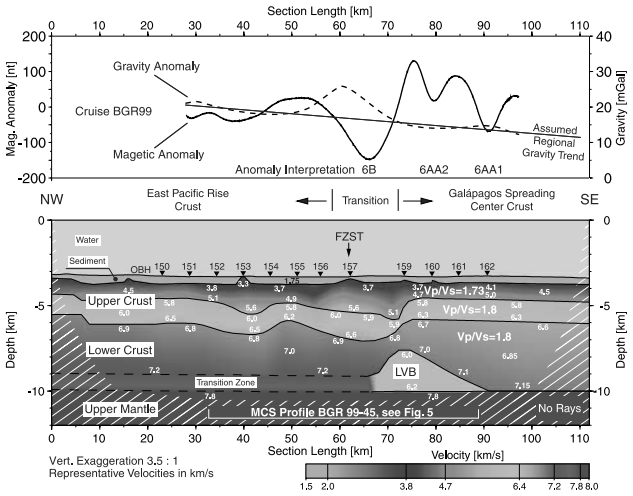

Figure 3. Crustal model for the wide-angle experiment off the Nicoya peninsula, Costa Rica. Velocities are displayed in grey-scale and for representative values in km/s. The hatched area is not resolved. In the upper part ship gravity with assumed regional trend and magnetic anomalies with interpretation (U. Barckhausen, per. com.) are shown, data collected on cruise BGR 99. LVB = Low Velocity Body; FZST = Fracture Zone Surface Trace, location after *Barckhausen et al.* [2001].

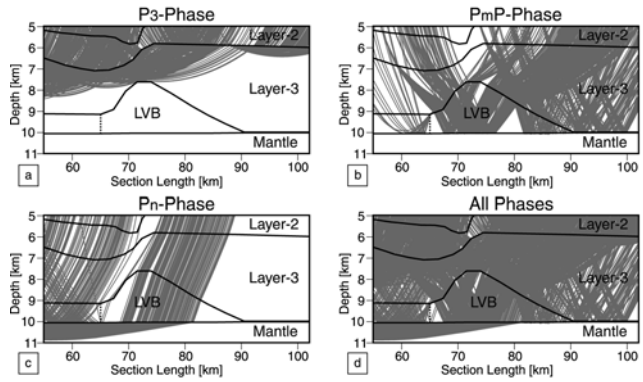

Figure 4. Detail of the crustal model with two-point rays traced for (a) P_3-phase, (b) P_mP-phase, (c) P_n-phase, and (d) all phases. The high ray coverage and good spacial distribution for the LVB and its vicinity underline the high resolution of this key model feature.

[10] The layer below is clearly identified as normal lower oceanic crust by seismic velocities ranging from 6.6 to 6.9 km/s at the top to 7.2 km/s at the base. Additionally, a mean layer thickness of 4 km and vertical gradients of 0.13 s^{-1} in the NW part of the section up to km 75 and 0.08 s^{-1} farther to the SE are within the range of normal oceanic lower crust. Within this layer a low-velocity body (LVB) from km 67 to 90 is an unusual anomaly. It is well constrained through 8 OBHs, OBH 154 to OBH 162, partly with reversed observations. The contribution of the individual phases P_3, P_mP, and P_n is shown by the two-point ray coverage in Figure 4. The P_3-phase defines its upper limit well, the lower boundary is constrained by the strong P_mP reflections that are clearly separated from P_3. The velocities of the LVB (6.0–6.2 km/s) are chosen such that they match the P_mP curvature and critical distances. All attempts with different velocities for the LVB and the lower crust in combination with a shifted Moho interface failed to verify the P_mP traveltimes or could not account for the observed separation of P_3 and P_mP.

[11] The Moho remains flat at 10 km depth throughout the section. The corresponding two-way traveltime varies little from ~7 s (Figure 5) and is perfectly matched at the SE section end by reflections on the adjacent MCS line BGR SO81-010 [*von Huene et al.*, 2000] (see Figure 1 for location). To account for the weak P_mP amplitudes recorded in the NW half of the section, a 1 km thick transition zone between crust and mantle is introduced as evident from synthetic amplitude modeling. The uppermost mantle velocity is 7.8 km/s.

[12] A zone of lateral inhomogeneity occurs near km 70 to 75 (OBH 159), where a sharp vertical displacement of all velocity contours occurs and coincides with the maximum thickness of the LVB. The adjacent section to the NW, up to the FZST at 62 km, is characterized by a 1 km thicker upper crust and by a smooth basement topography, contrasting with rougher basement to both sides (see blow-ups in Figure 5). The magnetic data show a prominent negative anomaly in this area and the gravity data a +9 mgal high. From OBH 159 to the SE, the model shows a uniform upper crust and vanishing LVB in the lower crust, ending at km 90 (OBH 162).

[13] S-wave modeling is based on the final P-wave model. The assignment of a constant Vp/Vs- (Poisson's) ratio for each crustal layer gives a satisfying fit to the observed seismic phases, taking picking uncertainties into account. Except for the uppermost crustal layer, which fits better with a 1.73 (Poisson's ratio = 0.25), the prevaling crustal Vp/Vs-ratio is 1.8 (Poisson's ratio = 0.28). This is in good agreement with the findings of *Miller and Christensen* [1997] for gabbroic rocks in oceanic crust.

[14] In Figure 5 we compare the two-way traveltime representation of the wide-angle model with the coincident MCS line BGR 99-45. No upper crustal reflectivity is found in the MCS data to match the clear indication for the division of the upper crust by the P_1 and P_2 wide-angle phases. An increasing reflectivity is observed from 6.0 to 6.7 s which coincides with the modeled lower crust. It is also apparent that this generally diffuse reflectivity is concentrated below the two major basement highs at km 40 and 62. The character of these basement highs, which are overlain by quasi continuous sedimentary sequences, indicates extrusive volcanic structures built on a young oceanic crust. In the wide-angle model it is evident, that these two locations show a thickened upper crust. We tend to interprete the lower crustal reflectivity as sills, which formed coherently to the basement highs in an early magmatic/

Table 1. Number of Picked Traveltimes, Assigned Picking Uncertainties and Achieved Rms-Traveltime Misfits

Traveltime branches	P_1	P_2	P_3	P_mP	P_n	All P	$S_1 + S_2$	S_3	All S
Traveltimes picked	297	1091	2129	285	1030	4832	584	1310	1894
Average pick uncertainties, ms	30	50	50–100	100–150	100	–	100	100	–
RMS misfit, ms	32	39	42	76	69	50	101	106	105

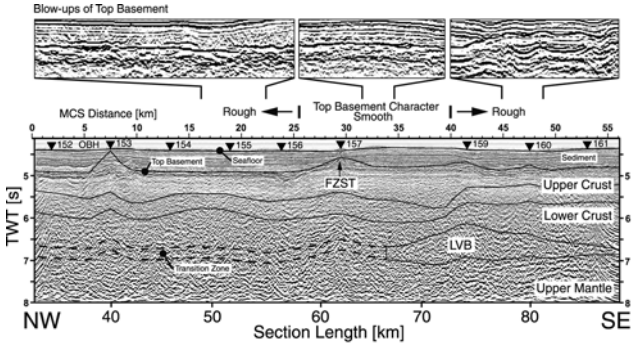

Figure 5. Poststack finite differences time-migrated sections of the BGR99-45 reflection line [*Barckhausen et al.*, 2001] coincident with the wide-angle section. The layer structure of the wide-angle model is superimposed by the thin solid lines. The transitional character of the Moho in the NW part of the section, as suggested by synthetic modeling, is marked by the two dashed lines. The three blow-ups show the lateral varying character of the top basement reflection.

volcanic event, most probable contemporaneous to plate breakup. The latter is indicated by the absence of any comparable volcanic structure SE of the FSZT on lines BGR 99-45 and BGR SO81-010. In the SE, from km 75 to the end. Two distinct reflective bands can be seen at 6.4 and 7.0 s TWT on the MCS line. They match top and bottom of the LVB and confirm the strong velocity contrast of this body to the adjacent crust and uppermost mantle.

[15] Two possible explanations for the LVB are considered in the following: serpentinized rock caused by uprising mantle getting in water contact during the plate breakup and remnants of a magma chamber.

[16] To test these two scenarios, we calculated the time differences for S-waves travelling through the given LVB for a basalt-gabbro or a serpentinite rock compositon, with the appropriate Vp/Vs ratios of 1.8 and 1.95, respectively. Unfortunately the calculated traveltime differences are within the traveltime uncertainties, therefore the S-wave observations cannot distinguish between the two alternatives. A second test relies on the gravity field. Serpentinites are generally less dense than gabbroic lower crustal rocks. Assuming a moderate lower serpentinite density of only -10 % for the LVB compared to the average (gabbroic) lower crust, an anomaly of -12 mgal would be expected. However, the ship gravity data show no corresponding deviation from the assumed regional trend (Figure 3). In addition, serpentinization would be accompanied by a considerable increase in volume, but neither crustal thickness nor Moho depth vary in the surrounding of this anomaly. Thus, we conclude that the LVZ cannot be interpreted by serpentinization. Another argument in favour of igneous rock is the clear limitation of the LVB which is proved by wide-angle and near-vertical reflection data. The sharp boundaries, and the flat lying Moho, are more easily explained by an intrusive igneous body than by the diffuse and variable-graded process of serpentinization.

4. Conclusions

[17] In summary, we find a normal oceanic crust at both ends of the section (NW of OBH 156/OBH 157 and SE of OBH 162). These parts represent, pure' EPR- and GSC-derived crust. Between these domains we find a zone of pronounced velocity variations including a LVB in the lower crust. In this area the distinctness of this body and the local gravity field point to an igneous intrusion rather than serpentinized rock. We see the forming of this body in context with the Farallon plate breakup ~23 Ma ago, which occurred somewhere between the FZST (near OBH 157) and OBH 159. The smooth basement topography, a thickened upper crust and a prominent magnetic anomaly indicate extensive lava flows. It remains open, as to what extent this region was formed anew or lavas flooded existing EPR crust, but the position and steep character of the northwestern LVB flank close to OBH 159 may indicate that EPR crust extends almost to this location. The overlying additional 1 km of basalt rocks and high temperatures during rifting may have significantly altered the original EPRs' magnetic pattern. The uniform upper oceanic crust, appearing from OBH 159 on to the SE, is the expression of the new spreading center and henceforth normal spreading process. With the growing of new crust the spreading center migrated to the SE, leaving GSC crust and part of the initial magma chamber behind in the NW.

[18] **Acknowledgments.** We are grateful to all colleagues and participants of the cruise SO144 1b, particularly to master H. Papenburg and his skillful crew of the RV SONNE. We thank U. Barckhausen for his comments on an earlier version. U. Barckhausen and the Bundesanstalt für Geowissenschaften und Rohstoffe (BGR) provided magnetic, gravity and seismic data of the line BGR 99-45. The PAGANINI project is funded by the German Ministry for Education and Research (BMBF) through grant 03G144A. Contribution No. 17 of SFB 574.

References

Barckhausen, U., C. R. Ranero, R. von Huene, S. C. Cande, and H. A. Roeser, Revised tectonic boundaries in the Cocos Plate off Costa Rica: Implications for the segmentation of the convergent margin and for plate tectonic models, *J. Geophys. Res.*, *106*(B9), 19,207–19,220, 2001.

Bialas, J., E. R. Flueh, G. Bohrmann, and Shipboard Scientific Party, FS Sonne, cruise report SO144/1&2, PAGANINI project, in *GEOMAR report*, GEOMAR, Kiel, Germany, 437 pp, 1999.

Fisher, R. L., Middle America Trench: Topography and structure, *Geol. Soc. Am. Bull.*, *72*, 703–720, 1961.

Hey, R. N., Tectonic evolution of the Cocos-Nazca spreading center, *Geological Society of America Bulletin*, *88*, 1414–1420, 1977.

Kimura, G., E. Silver, P. Blum, and S.S. Party, *Proceedings of the Ocean Drilling Program Initial Reports*, *170* (Ocean Drilling Program, College Station, Tex.), 1997.

Lonsdale, P., and K. D. Klitgord, Structure and tectonic history of the eastern Panama Basin, *Geological Society of America Bulletin*, *89*, 981–999, 1978.

Miller, D. J., and N. I. Christensen, Seismic velocities of lower crustal and upper mantle rocks from the slow-spreading Mid-Atlantic Ridge, south of the Kane transfrom zone (MARK), *Proceedings of the Ocean Drilling Program*, edited by J. A. Karson, M. Cannat, J. D. Miller, and D. Elthon, (Scientific Results), 437–453, 1997.

Smith, W. H. F., and D. T. Sandwell, Global sea floor topography from satellite altimetry and ship depth soundings, *Science*, *277*, 1956–1962, 1997.

von Huene, R., J. Bialas, E. Flueh, B. Cropp, T. Csernok, E. Fabel, J. Hoffmann, K. Emeis, P. Holler, G. Jeschke, M. Leandro, M. Perez Fernandez, J. S. Chavarria, H. Florez, D. Z. Escobedo, R. Leon, and O. L. Barrios, Morphotectonics of the Pacific convergent margin of Costa Rica, *Geologic and Tectonic Development of the Caribbean Plate Boundary in Southern Central America*, *295*, 291–307, 1995.

von Huene, R., C. Ranero, W. Weinrebe, and K. Hinz, Quaternary convergent margin tectonics of Costa Rica, segmentation of the Cocos Plate, and Central American volcanism, *Tectonics*, *19*, 314–334, 2000.

Christian Walther and Ernst Flueh, GEOMAR Research Center for Marine Geosciences, Kiel, Germany.